# Caveolin Cycles between Plasma Membrane Caveolae and the Golgi Complex by Microtubule-dependent and Microtubule-independent Steps

**Patricia A. Conrad, Eric J. Smart, Yun-Shu Ying, Richard G.W. Anderson, and George S. Bloom**

Department of Cell Biology and Neuroscience, University of Texas Southwestern Medical Center, Dallas, Texas 75235

***Abstract.*** Caveolin is a protein associated with the characteristic coats that decorate the cytoplasmic face of plasma membrane caveolae. Recently it was found that exposure of human fibroblasts to cholesterol oxidase (CO) rapidly induces caveolin to redistribute to the ER and then to the Golgi complex, and that subsequent removal of CO allows caveolin to return to the plasma membrane (Smart, E. J., Y. -S. Ying, P. A. Conrad, R. G. W. Anderson. *J. Cell Biol.* 1994. 127:1185–1197). We now present evidence that caveolin normally undergoes microtubule-dependent cycling between the plasma membrane and the Golgi. In cells that were treated briefly with nocodazole and then with a mixture of nocodazole plus CO, caveolin relocated from the plasma membrane to the ER and then to the ER/Golgi intermediate compartment (ERGIC), but subsequent movement to the Golgi was not observed. Even in the absence of CO, nocodazole caused caveolin to accumulate in the ERGIC. Nocodazole did not retard the movement of caveolin from the Golgi to the plasma membrane after removal of CO. Incubation of cells at 15° followed by elevation of the temperature to 37° caused caveolin to accumulate first in the ERGIC and then in the Golgi, before finally reestablishing its normal steady state distribution predominantly in plasma membrane caveolae. In cells released from a 15° block, movement of caveolin from the Golgi to the plasma membrane was not inhibited by nocodazole. Taken together, these results imply that caveolin cycles constitutively between the plasma membrane and the Golgi by a multi-step process, one of which, ERGIC-to-Golgi transport, requires microtubules. This novel, bidirectional pathway may indicate roles for microtubules in the maintenance of caveolae, and for caveolin in shuttling fatty acids and cholesterol between the plasma membrane and the ER/Golgi system.

In fibroblasts and many other cell types, microtubules (MTs)[1] radiate outward from a perinuclear MT-organizing center (MTOC), with their minus ends anchored at the MTOC and their plus ends facing the cell periphery. MTs oriented in this manner serve as intracellular "highways" along which tubulovesicular transport intermediates of the secretory and endocytic pathways travel between the cell center, where the Golgi complex and lysosomes are located, and the plasma membrane, where materials are exchanged between the extracellular environment and the cytoplasm. As a consequence of their radial organization in the cell and their involvement in endomembrane transport, MTs are responsible for maintaining the normal intracellular locations and organization of numerous quasi-stable membrane systems, including the ER (30), the Golgi (8, 18, 31, 33), and late endosomes and lysosomes (13, 22, 29).

By comparison, little has been known about the role of MTs in maintaining the structure and localization of caveolae. These flask-shaped invaginations of the plasma membrane, typically 50–100 nm in diameter, have been observed in most cell types and evidently serve multiple functions. Classically, caveolae have been known for their involvement in transcytosis in endothelial cells (14). More recently, they were identified as the sites for folic acid uptake by a process called potocytosis (1, 2). During potocytosis the caveola undergoes an internalization cycle that involves formation of a closed compartment called a plasmalemmal vesicle, release of folic acid into the cytoplasm and reformation of an open caveola. There is evidence that caveolae have a high concentration of glycolipids, sphingomyelin, and cholesterol (4, 28), as well as a protein called caveolin (19). They are also the collecting sites for multiple glycosylphosphatidylinositol (GPI)-anchored membrane proteins (5, 35). The recent finding that isolated caveolae contain a variety of signal transducing molecules (5, 12, 21, 26) suggests that, in addition, they play a role in cell signaling (1).

A totally unexpected aspect of caveolar behavior was

Address all correspondence to George S. Bloom, University of Texas Southwestern Medical Center, Department of Cell Biology and Neuroscience, 5323 Harry Hines Boulevard, Dallas, TX 75235. Tel.: (214) 648-7680. Fax: (214) 648-9160/8694. e-mail: bloom@utsw.swmed.edu

1. *Abbreviations used in this paper*: CO, cholesterol oxidase; ERGIC, ER/Golgi intermediate compartment; GPI, glycosylphosphatidylinositol; LDL, low density lipoprotein; MT, microtubule; MTOC, microtubule organizing center.

recently revealed by studies of human fibroblasts that had been incubated with the membrane impermeable enzyme, cholesterol oxidase (CO), which caused oxidation of cholesterol in caveolae (28). Localization of caveolin with a monoclonal antibody revealed immunoreactive protein to be mainly in caveolae in unperturbed cells. In cells treated with CO, however, caveolin redistributed to the Golgi apparatus. Caveolin first appeared in the rough ER during CO-induced transport, and then migrated to the Golgi. Subsequent removal of CO quickly led to the return of caveolin to caveolae. In contrast to the striking effects of CO on caveolin, CO did not alter the morphology or number of caveolae in any obvious manner (28). It appears, therefore, that CO does not induce intact caveolae to move to the Golgi.

The effects of CO on caveolin traffic raised several important questions, two of which are addressed in the current report. First, are MTs required for the inward movement of caveolin in CO-treated cells or the outward movement of caveolin that follows CO removal? Second, did CO reveal a normal cyclic transport pathway for caveolin between the cell surface and the Golgi, or alternatively, did it artifactually induce a redistribution of caveolin to an ectopic location? These questions were addressed by immunofluorescence and immunoelectron microscopy, and biochemical analysis of normal human fibroblasts that had been perturbed chemically with CO and the MT-depolymerizing drug, nocodazole, and physically by exposure to 15°. The net results indicate that caveolin does, indeed, cycle constitutively between caveolae and the Golgi, and that the inward, but not the outward movement requires MTs. This study provides the first evidence that MTs are needed to maintain the normal distribution of a resident caveolar protein, and also reveals a novel, bidirectional pathway for the exchange of materials between the plasma membrane and the Golgi complex. Caveolin may follow this pathway to shuttle lipids and cholesterol between the cell surface and the ER/Golgi membrane system.

## Materials and Methods

### Materials

Materials were purchased from the following sources: DME, glutamine, trypsin-EDTA, and penicillin/streptomycin: GIBCO BRL (Gaithersburg, MD); FBS: Hazleton Research Products, Inc. (Lenexa, KS); cholesterol oxidase (from *Nocardia erythropolis*): Boehringer Mannheim (Indianapolis, IN); nocodazole, trypsin, soybean trypsin inhibitor, and DABCO (1,4-diazabicyclo-(2,2,2) octane): Sigma Chem. Co. (St. Louis, MO); Percoll: Pharmacia LKB Biotechnology (Piscataway, NJ); Fluoromount G: Southern Biotechnology Associates, Inc. (Birmingham, AL); "SuperSignal" chemiluminescent reagent: Pierce (Rockford, IL); HRP-labeled goat anti–mouse IgG, and TRITC-goat anti–mouse IgG: Cappel (West Chester, PA), FITC-goat anti–mouse IgM: Zymed Laboratories (San Francisco, CA); FITC-goat anti–rabbit IgG and CY5-donkey anti–rabbit IgG: Jackson ImmunoResearch Labs (West Grove, PA); goat anti–mouse IgG conjugated to 10 nm gold: Energy Beam Sciences (Agawam, MA).

The following primary antibodies were generously provided as gifts: a monoclonal mouse IgG against caveolin (mAb 2234) from Dr. John Glenney of Glentech, Inc. (Lexington, KY) (19); a polyclonal rabbit antiserum against human galactosyltransferase from Dr. Eric Berger of the University of Zurich (Zurich, Switzerland) (3); polyclonal rabbit antisera against the EAGE peptide of β-COP from Drs. Thomas Kreis of the University of Geneva (Geneva, Switzerland) (17) and Jennifer Lippincott-Schwartz of the NIH (Bethesda, MD) (10); a monoclonal mouse IgG specific for ERGIC-53 from Dr. Hans-Peter Hauri of the University of Basel (Basel, Switzerland) (23); a polyclonal rabbit antiserum against the human low density lipoprotein (LDL) receptor from Dr. Joseph Goldstein of UT Southwestern; a polyclonal antibody against cathepsin D from Dr. William Brown of Cornell University (15). In addition, a monoclonal mouse IgM against tubulin (34) was obtained from hybridoma cells grown in the Bloom laboratory.

### Cell Culture

Human fibroblasts were derived from a skin biopsy obtained from a normal patient, and were grown in monolayer culture in DME supplemented with penicillin/streptomycin and 10% FBS. For the temperature block experiments, cells were incubated for 2 h at 15° in DME +20 mM Hepes at pH 7.4, and then were returned to 37°. Nocodazole was diluted from a 10-mM stock in DMSO, and was used at a final concentration of 40 μM. CO was used at a final concentration of 0.5 U/ml (1 U of activity converts 1 μmol of cholesterol to cholestenone in 1 min).

### Immunofluorescence and Immunoelectron Microscopy

All procedures for indirect immunofluorescence were performed at room temperature, 0.1 M phosphate buffer at pH 7.2, was used for all rinse steps, and all primary and secondary antibodies were diluted into phosphate buffer containing 10 mg/ml BSA. Cells grown on glass coverslips were fixed for 30 min in phosphate buffer containing 4% ρ-formaldehyde, and permeabilized with 0.05% Triton X-100 in phosphate buffer for 2 min. Incubations with primary and secondary antibodies were for 30 min each. For double and triple immunofluorescence experiments, the primary and secondary antibodies were mixed together for the first and second incubation steps, respectively. For double immunofluorescence, the primary antibodies were mouse monoclonal IgG against caveolin or ERGIC-53, and rabbit polyclonal anti–β-COP, anti-cathepsin D or anti-LDL receptor; and the secondary antibodies were TRITC-goat anti–mouse IgG and FITC-goat anti–rabbit IgG. For triple immunofluorescence, the primary antibodies were mouse anti-caveolin (monoclonal IgG), mouse anti-tubulin (monoclonal IgM) and rabbit polyclonal anti–β-COP, and the secondary antibodies were TRITC-goat anti–mouse IgG, FITC-goat anti–mouse IgM and CY5-donkey anti–rabbit IgG. Coverslips were mounted on glass slides using Fluoromount G +2.5% DABCO.

Procedures for immuno-EM localization of caveolin and β-COP were exactly as described previously (28). All immunofluorescence and immuno-EM experiments were performed as detailed time courses in which several antigens were localized at each time point. For example, cells were fixed after a 2-h incubation at 15°, and after subsequent transfer to 37°, every 5 min for 2 h. At each time point in this case, cells were examined by double or triple immunofluorescence for caveolin, β-COP, ERGIC-53, galactosyltransferase, and tubulin. For the temperature block reversal, and for all other time course experiments, immunofluorescence and immunoelectron micrographs of cells at selected time points are shown in the figures.

### Biochemical Characterization of Caveolin in Isolated Subcellular Fractions

The relative levels of caveolin in cytosol, plasma membrane, and intracellular membranes were determined by immunoblotting of fractions isolated from cells cultured in 10 × 100-mm dishes in medium containing or lacking nocodazole. The procedure is based on an earlier study in which caveolin distributions were analyzed in cells that had been cultured in medium containing or lacking CO (27). In the present case, cells were treated with 50 μg/ml cycloheximide for 2 h, during the last hour of which 40 μM nocodazole or an equivalent volume of DMSO was also present. Next, each set of cells was collected by scraping, and was homogenized in 1 ml buffer A (0.25 M sucrose, 1 mM EDTA, 20 mM tricine at pH 7.8) using a 2-ml Wheaton tissue grinder (catalogue number 084146A). Each homogenate was then centrifuged for 10 min at 1,000 *g* in an Eppendorf microcentrifuge. The resulting postnuclear supernatant was stored on ice, and the pellet was homogenized and centrifuged exactly as was done earlier for the cells. The original and new postnuclear supernatants were combined, layered on top of 23 ml of 30% Percoll in buffer A, and centrifuged at 29,000 rpm (84,679 $g_{max}$) for 30 min at 4° in a 60 Ti rotor (Beckman Instrs., Fullerton, CA). This centrifugation step yielded a layer of cytosol on top of the Percoll gradient, and two membrane fractions within the gradient. The low density fraction contained highly purified plasma membrane, while Golgi, ER, lysosomal, endosomal, and mitochondrial membranes

were present throughout the high density peak (27). Aliquots of cytosol, plasma membrane and intracellular membranes were collected from the Percoll gradient, and analyzed by SDS-PAGE (9) using 12.5% polyacrylamide gels, and by immunoblotting (27, 32) with anti-caveolin. Each gel lane contained 50 μg of protein, the secondary antibody was HRP-conjugated goat anti–mouse IgG, and Pierce SuperSignal chemiluminescent substrate was used to detect immunoreactive caveolin.

To analyze the accessibility of caveolin to trypsin in subcellular fractions obtained from control and nocodazole-treated cells, postnuclear supernatants were prepared exactly as described in the prior paragraph, except that 1× 100-mm culture dish was used per experiment. Each postnuclear supernatant was centrifuged at 43,000 rpm (100,000 $g_{max}$) for 1 h at 4° in a Beckman 100.3 rotor, yielding a 1-ml supernatant (soluble fraction) and a pellet (particulate fraction), which was resuspended in 1 ml buffer A. Each fraction was then incubated for 30 min on ice in the presence or absence of 300 μg/ml trypsin, after which soybean trypsin inhibitor was added to 300 μg/ml. Finally, each sample was precipitated with TCA (~7% final concentration), resuspended in 25 μl sample buffer for SDS-PAGE, and analyzed by SDS-PAGE and Western blotting as described in the previous paragraph.

## Results

Throughout this study it was necessary to stain cells for double immunofluorescence using a monoclonal IgG antibody to caveolin and appropriate polyclonal antibodies in order to identify membrane compartments with which caveolin was associated. The polyclonal antibody that was most extensively used was specific for the coatomer protein, β-COP (6, 25). Anti–β-COP stained both the Golgi and punctate membranes scattered throughout the cytoplasm of normal human fibroblasts cultured in control medium (see Figs. 2 *B* and 4 *B*). The punctate structures were also labeled in control cells by a monoclonal antibody to ERGIC-53 (data not shown), an integral membrane protein of the ER/Golgi intermediate compartment, or ERGIC (23). Partial colocalization of β-COP with an ERGIC marker protein is consistent with prior reports that β-COP is found on a membrane compartment through which the transmembrane glycoprotein of vesicular stomatitis virus passes after leaving the ER and before entering the Golgi (6, 10). By definition, this compartment is the ERGIC (24).

In cells that were treated for 1 h with 40 μM nocodazole, β-COP, and ERGIC-53 remained partly colocalized. Antibodies to both proteins stained the ERGIC, while anti–β-COP also labeled Golgi fragments that resulted from MT disassembly (Fig. 1, *A* and *B*). After incubation of cells at 15° for 2 h, which reportedly causes partial redistribution of ERGIC-53 to the Golgi (24), antibodies to either β-COP or ERGIC-53 stained both the perinuclear Golgi and the widely scattered ERGIC membranes (Fig. 1, *C* and *D*). Double labeling of cells with antibodies to β-COP and the integral membrane Golgi marker, galactosyltransferase, or with ERGIC-53 and galactosyltransferase, demonstrated unambiguous distinctions between the distributions of Golgi and ERGIC membranes under all culture conditions used in this study (not shown). We concluded, therefore, that anti–β-COP could be used to visualize the Golgi and the ERGIC in normal human fibroblasts cultured under a variety of conditions.

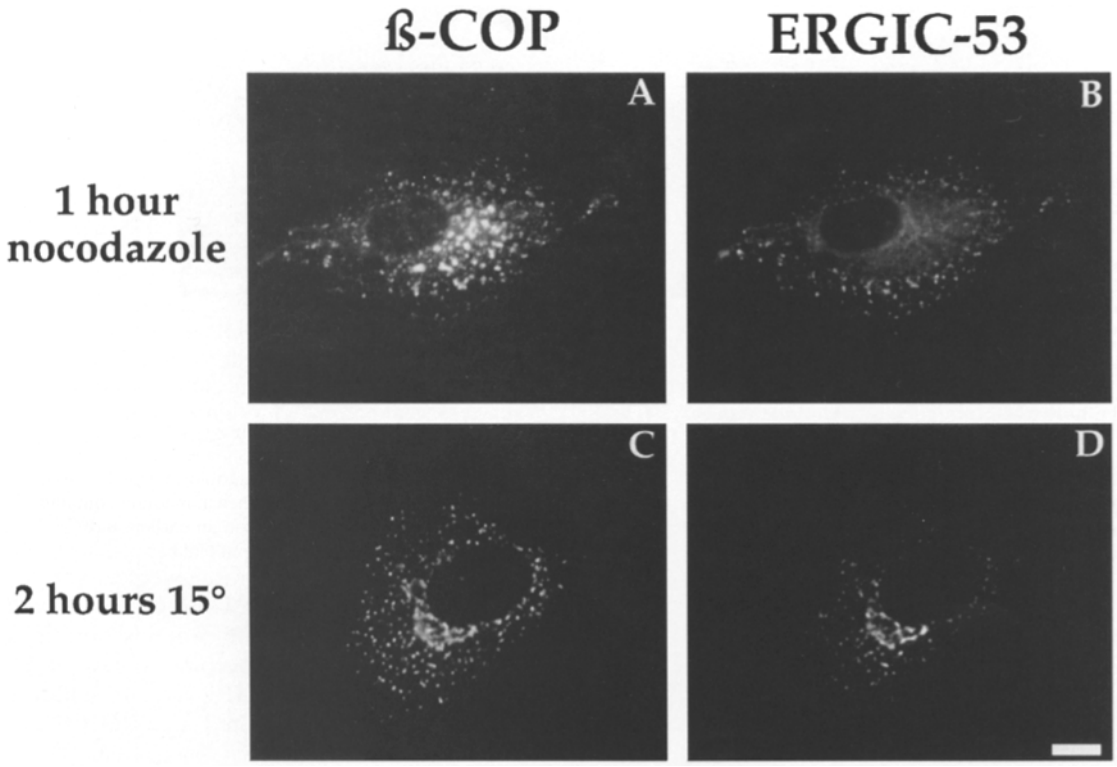


*Figure 1.* β-COP is a marker for the Golgi and the ERGIC. Normal human fibroblasts were grown for 1 h in the presence of 40 μM nocodazole (*A* and *B*) or for 2 h at 15° before being fixed and stained for double immunofluorescence using antibodies to β-COP (*A* and *C*) and ERGIC-53 (*B* and *D*). Note the extensive colocalization of β-COP and ERGIC-53 on punctate ERGIC membranes scattered throughout the cytoplasm in both sets of micrographs. In the nocodazole-treated cell, β-COP (*A*), but not ERGIC-53 (*B*) can be seen on Golgi fragments located predominantly to the right of the nucleus. In the cell incubated at 15°, both β-COP (*C*) and ERGIC-53 (*D*) can be seen at the Golgi apparatus, which is adjacent to the lower left edge of the nucleus. The bar in panel *D* equals 10 μm.

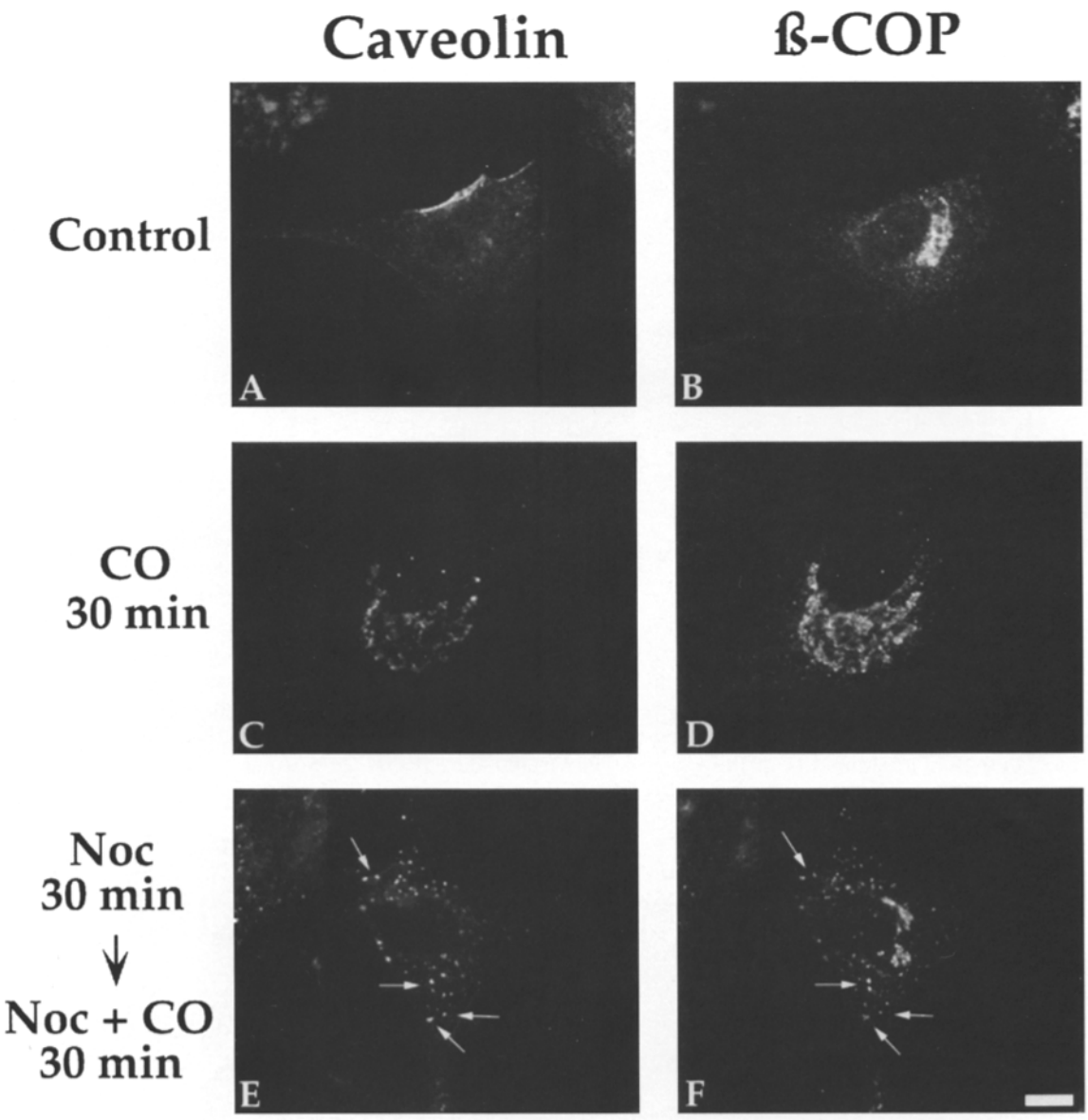


*Figure 2.* CO-induced movement of caveolin to the Golgi requires MTs. The distributions of caveolin and β-COP are shown by double immunofluorescence in normal human fibroblasts grown in control medium (*A* and *B*), in the presence of CO for 30 min (*C* and *D*), and in the presence of 40 μM nocodazole for 30 min followed by a mixture of 40 μM nocodazole plus CO (*E* and *F*). Note that caveolin was able to reach the Golgi in the cell treated with CO alone (compare *C* and *D*). When cells were pretreated with nocodazole to depolymerize MTs, however, caveolin accumulated at β-COP–positive ERGIC membranes (*arrows*), but not at the β-COP–positive Golgi. The bar in panel *F* equals 10 μm.

### *MTs Are Required for CO-induced Transport of Caveolin to the Golgi*

To determine whether MTs are required for movement of caveolin to the Golgi in CO-treated human fibroblasts, cells were cultured in the presence or absence of nocodazole before being exposed to CO. The cells were then stained for double immunofluorescence with monoclonal anti-caveolin and polyclonal anti–β-COP. In control cells, the distributions of caveolin and β-COP did not overlap (Fig. 2, *A* and *B*). Caveolin was most concentrated in discrete patches at the plasma membrane, while β-COP was found on the Golgi and on widely distributed, punctate membranes of the ERGIC. Despite their distinct distributions in control cells, caveolin and β-COP were extensively colocalized in cells treated with 0.5 U/ml CO for 30 min (Fig. 2, *C* and *D*). In such cells, both proteins were most abundant at the Golgi, which had become somewhat distended as a result of exposure to CO (28). In addition, β-COP, but not caveolin, was detected on ERGIC membranes in CO-treated cells.

Although CO consistently induced movement of caveolin to the Golgi in cells that were not exposed to other perturbants, pretreatment of cells with nocodazole blocked this movement (Fig. 2, *E* and *F*). After a 30-min incubation in 40 μM nocodazole, which completely depolymerized MTs (data not shown), CO was added to the nocodazole-

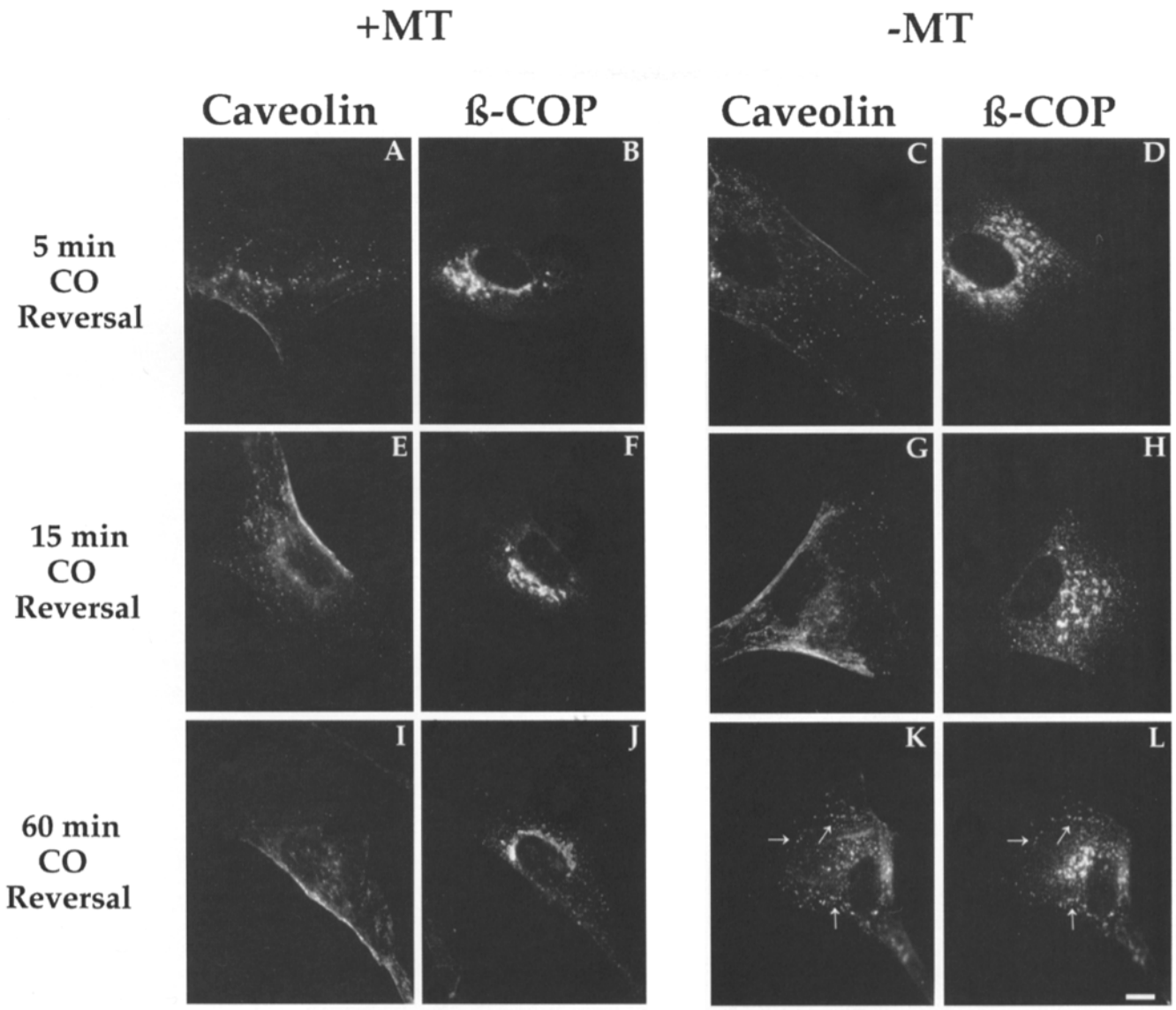


*Figure 3.* MTs are not required for movement of caveolin from the Golgi to the plasma membrane after removal of CO. Normal human fibroblasts were exposed to CO for 30 min to redistribute caveolin to the Golgi, and then were cultured for an additional 20 min with CO in the presence of 40 μM nocodazole, and finally were placed in CO-free medium containing 40 μM nocodazole. After further incubations of 5, 15, and 60 min, cells were fixed and stained for double immunofluorescence using antibodies to caveolin and β-COP (−MTs). For comparison, another set of cells was never exposed to nocodazole, but otherwise was treated identically (+MTs). In either the presence or absence of MTs, most of the caveolin had exited the Golgi within 5 min of CO reversal (*A–D*). The caveolin at this time point was predominantly in vesicle-like structures that did not colocalize with β-COP, and therefore were not part of the ERGIC. Some caveolin was also present at the plasma membrane 5 min after CO was removed (*A* and *C*). By 15 min of CO reversal, the majority of the caveolin in cells containing or lacking MTs appeared to be at the plasma membrane, although some caveolin was still present on β-COP–negative vesicles (*E–H*). After 60 min in CO-free medium, nearly all of the caveolin was at the plasma membrane in cells that contained MTs (*I*), but in cells that lacked MTs, caveolin was most concentrated in β-COP–positive ERGIC membranes (*K* and *L*; see arrows). The bar in panel *L* equals 10 μm.

containing medium to a final concentration of 0.5 U/ml. In cells that were fixed 30 min later, the Golgi remained partially intact near the cell center, as evidenced by staining with anti–β-COP, which also labeled widely scattered punctate membranes of the ERGIC. The caveolin in such cells was not localized at the Golgi, but instead was restricted to the ERGIC. Thus, in cells that lacked MTs, caveolin accumulated in the ERGIC and was unable to move to the Golgi in response to CO.

### *MTs Are Not Required for Movement of Caveolin from the Golgi to the Plasma Membrane after Removal of CO*

To determine whether MTs are involved in moving caveolin to the cell surface following CO removal, it was necessary first to accumulate caveolin at the Golgi using CO, then to disassemble MTs, and finally to remove the CO. This was accomplished by treating cells with 0.5 U/ml CO for 30 min, then with 0.5 U/ml CO plus 40 μM nocodazole for 20 min, and finally with CO-free medium containing or lack-

ing 40 μM nocodazole. At various times thereafter, cells were fixed and stained for double immunofluorescence with antibodies to caveolin and β-COP. MTs were not observed in cells that were maintained in nocodazole after CO reversal, but extensive MT networks were found in cells within 10 min after removal of both nocodazole and CO (data not shown).

Within 5 min after CO was removed from cells containing or lacking MTs, caveolin had exited the Golgi and was present primarily in punctate structures that did not colocalize with ERGIC/Golgi membranes stained by anti–β-COP. Some staining of the plasma membrane by anti-caveolin was also seen after 5 min of CO reversal, whether or not MTs were present (Fig. 3, *A–D*). In both MT-containing and MT-depleted cells, the majority of the caveolin appeared to be at the plasma membrane 15 min after removal of CO, with the remainder being present on β-COP–negative vesicles (Fig. 3, *E–H*). After 60 min of CO reversal, nearly all caveolin in MT-containing cells was at the cell surface (Fig. 3 *I*). In contrast, 60 min after CO was removed from cells lacking MTs, caveolin was found predominantly in the cytoplasm on punctate structures that colocalized with β-COP, and to a lesser extent at the plasma membrane (Fig. 3, *K* and *L*). These results indicated that after CO removal, MTs are not necessary for caveolin to move from the Golgi to the plasma membrane, but are required for caveolin to accumulate there preferentially. In the absence of MTs, far more caveolin accumulated in the ERGIC/Golgi than at the plasma membrane.

### *Caveolin Redistributes to the ERGIC after Treatment of Cells with Nocodazole Alone*

The observed accumulation of caveolin in the ERGIC/Golgi after removal of CO from nocodazole-treated cells (see Fig. 3) suggested that the normal steady-state enrichment of caveolin in caveolae is sensitive not only to cholesterol oxidation by CO, but to disassembly of MTs as well. To test this idea, the distributions of caveolin and β-COP were examined by double immunofluorescence in cells that had been treated with nocodazole alone.

Before nocodazole addition, caveolin was located primarily at the cell surface, while β-COP was most prominent at the Golgi, but was also evident on widely dispersed ERGIC membranes (Fig. 4, *A* and *B*; also see Fig. 2, *A* and *B*). Within 30 min of exposure to 40 μM nocodazole, caveolin colocalized with β-COP at peripherally distributed membranes of the ERGIC, and was also detectable at the plasma membrane. The Golgi complex remained partially intact near the cell center under these conditions, as indicated by the antibody to β-COP, but caveolin was not detectable at the Golgi (Fig. 4, *C* and *D*). Caveolin and β-COP remained extensively colocalized after 90 min of nocodazole treatment, at which point caveolin was nearly gone from the

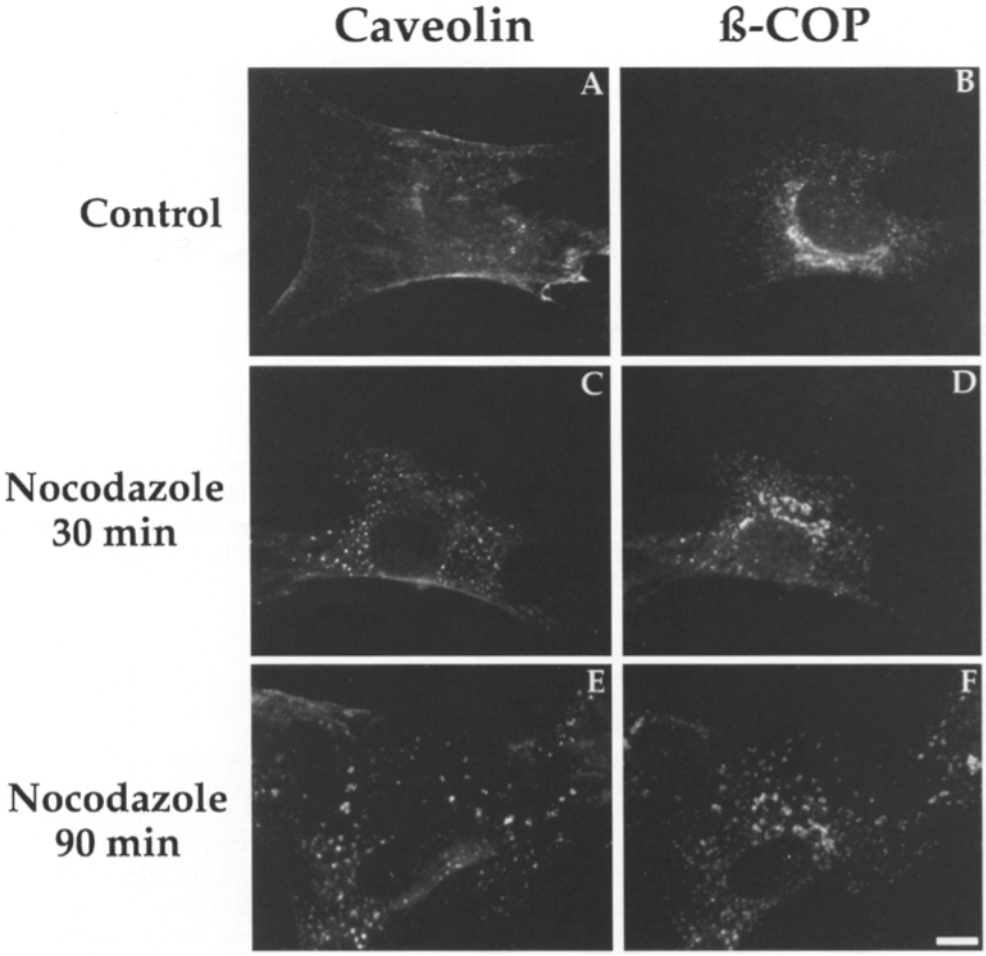


*Figure 4.* Nocodazole induces caveolin to redistribute from the plasma membrane to the ERGIC. The distributions of caveolin and β-COP are shown by double immunofluorescence in normal human fibroblasts grown in control medium (*A* and *B*), and in the presence of 40 μM nocodazole for 30 (*C* and *D*), or 90 (*E* and *F*) min. Note that caveolin redistributed from its control location at the plasma membrane (*A* and *B*) to β-COP–positive ERGIC membranes in nocodazole-treated cells (*C–F*). Residual Golgi membranes located near the nuclei of the nocodazole-treated cells were stained by anti–β-COP, but not by anti-caveolin. The bar in panel *F* equals 10 μm.

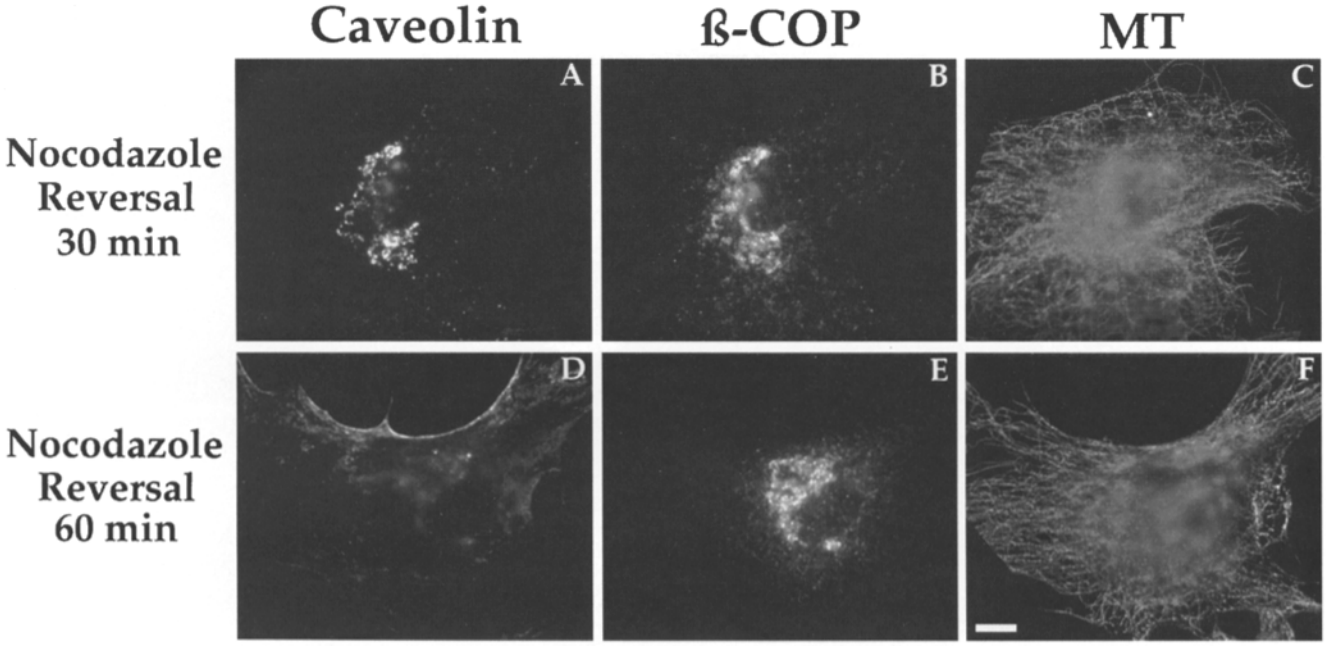


*Figure 5.* Removal of nocodazole induces caveolin to redistribute from the ERGIC to the plasma membrane after passing through the Golgi. The distributions of caveolin, β-COP and tubulin (MT) are shown by triple immunofluorescence in normal human fibroblasts cultured in the presence of 40 μM nocodazole for 1 h before transfer to nocodazole-free medium. Within 30 min of nocodazole reversal, by which time MTs were abundant (*C*), caveolin migrated from the ERGIC (see Fig. 4) to the β-COP–positive Golgi (*A* and *B*). After 60 min in the absence of nocodazole, caveolin returned to its normal steady-state location predominantly at the plasma membrane (*D*). The bar in panel *F* equals 10 μm.

plasma membrane and only small, β-COP–positive remnants of the Golgi remained near the nucleus. Anti-caveolin did not stain the residual Golgi membranes (Fig. 4, *E* and *F*). These observations demonstrate that caveolin redistributes from the plasma membrane to the ERGIC after disassembly of MTs. Moreover, they imply that after removal of CO from nocodazole-treated cells, caveolin moved from the Golgi to the plasma membrane, and then to the ERGIC (see Fig. 3).

### *Nocodazole Reversal Causes Caveolin to Move Synchronously from the ERGIC to the Golgi, and then to the Plasma Membrane*

To determine whether the effects of MT disassembly on caveolin were reversible, cells were treated with 40 μM nocodazole for 1 h, after which they were transferred to nocodazole-free medium. At 10-min time intervals thereafter, cells were fixed and stained for triple immunofluorescence using antibodies to caveolin, β-COP, and tubulin.

Fig. 5 illustrates the results of a typical experiment 30 and 60 min after removal of nocodazole. At the 30-min time point, when the MT network had fully reformed, caveolin was most concentrated near the cell center, where it was extensively colocalized with β-COP at the Golgi (Fig. 5, *A–C*). In contrast, caveolin and β-COP were not colocalized at 60 min of nocodazole reversal. Whereas caveolin had returned to the plasma membrane, β-COP was still most abundant at the Golgi (Fig. 5, *D–F*). Taken together, these results demonstrate that the effects of nocodazole on the distribution of caveolin are fully reversible, but that caveolin does not return directly to the plasma membrane from the ERGIC after removal of nocodazole. Instead, caveolin travels from the ERGIC to the Golgi, before completing its journey back to plasma membrane caveolae.

### *Caveolin Moves Reversibly from the Plasma Membrane to the Golgi after Release of Cells from a 15° Temperature Block*

To test the possibility that CO and nocodazole act by imposing reversible roadblocks along a pathway that is normally followed by caveolin in unperturbed cells, a third potential perturbant of caveolin, incubation of cells at 15°, was investigated. It is well established that materials which normally move to the Golgi are effectively blocked at pre-Golgi sites when cells are held at 15°, and move en masse to the Golgi and beyond after the cells are returned to 37° (10, 20, 24).

Shown in Fig. 6 are the results of a temperature block experiment, in which cells were double labeled with antibodies to caveolin and β-COP. After cells were incubated at 15° for 2 h, caveolin was still localized primarily at the plasma membrane, and β-COP was found both on the centrally located Golgi and throughout the ERGIC (Fig. 6, *A* and *B*). Compared to unperturbed cells (see Figs. 2 *B* and 4 *B*), these temperature blocked cells contained Golgi complexes that were diminished in size, and staining of ERGIC membranes by anti–β-COP was enhanced. When the cells were transferred to 37°, most of the detectable caveolin moved to the ERGIC within 10 min, at which point the distribution of β-COP had not yet changed appreciably (Fig. 6, *C* and *D*). After 30 min at 37°, however, both caveolin and β-COP had moved to the Golgi, the morphology of which appeared to have fully recovered from the temperature block (Fig. 6, *E* and *F*). Within an hour of

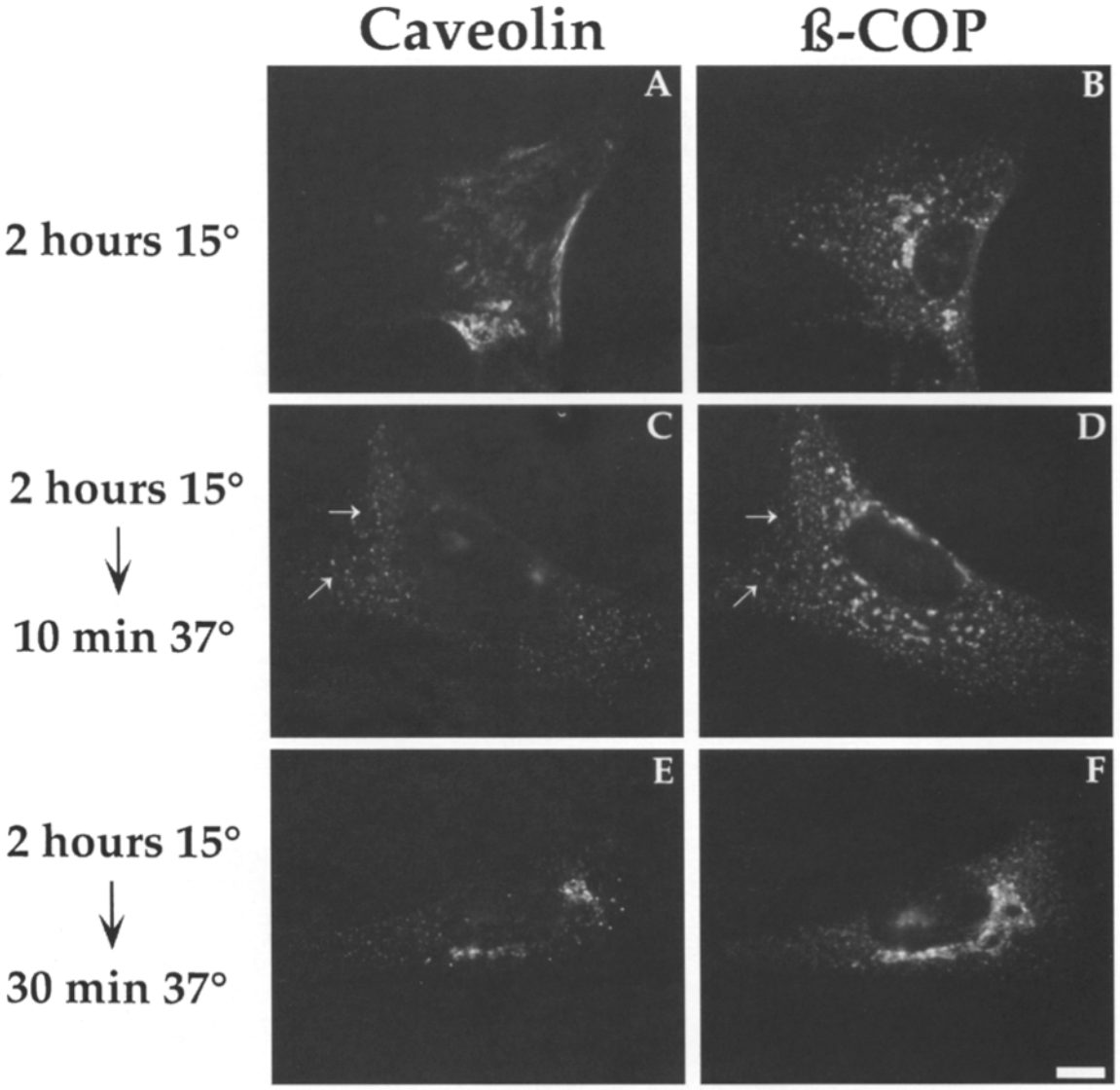


*Figure 6.* Release of cells from a cold block at 15° induces caveolin to move from the plasma membrane to the ERGIC, and then to the Golgi. The distributions of caveolin and β-COP are shown by double immunofluorescence in normal human fibroblasts that were incubated for 2 h at 15° before transfer to 37°. Immediately after the cold block, most of the caveolin was located at the plasma membrane (*A*), and the β-COP–positive Golgi was somewhat fragmented (*B*). After 10 min at 37°, caveolin was virtually absent from the plasma membrane, and colocalized with β-COP at ERGIC membranes (*C* and *D*; see arrows), but not at the Golgi, which remained fragmented. After a 30-min incubation at 37°, most of the caveolin moved to the β-COP–positive Golgi, which now appeared relatively intact (*E* and *F*). The bar in panel *F* equals 10 μm.

recovery at 37°, caveolin returned to the plasma membrane.

When cells were held at 15° for 2 h, and were then incubated at 37° sufficiently long to permit synchronous transport of caveolin to the Golgi, subsequent addition of nocodazole did not block movement of caveolin back to the plasma membrane. In contrast, when nocodazole was added at the same time as the shift to 37°, caveolin remained in the ERGIC and did not reach the Golgi (data not shown). Based on these collective results, we conclude that temporary incubation of cells at 15°, like transient exposure of cells to CO or nocodazole, reveals a cyclic trafficking pathway for caveolin that leads from the plasma membrane to the Golgi via the ER and ERGIC, and then from the Golgi back to plasma membrane. Moreover, as was found for addition and removal of CO (see Figs. 2 and 3), MTs are required for transport of caveolin from the ERGIC to the Golgi, but not for the return of caveolin from Golgi to the plasma membrane after release of cells from a 15° temperature block.

### *Characterization of the Caveolin Trafficking Cycle by Immuno-EM*

The caveolin internalization cycle was confirmed by immunogold EM, as shown in Fig. 7. Nearly all of the caveolin in control cells grown at 37° was in caveolae. Only a few gold particles were seen scattered in the lumen of the rough ER, in tubulovesicular organelles, or in the Golgi (Fig. 7 *A*). Caveolin was still primarily in caveolae after 2 h at 15°,

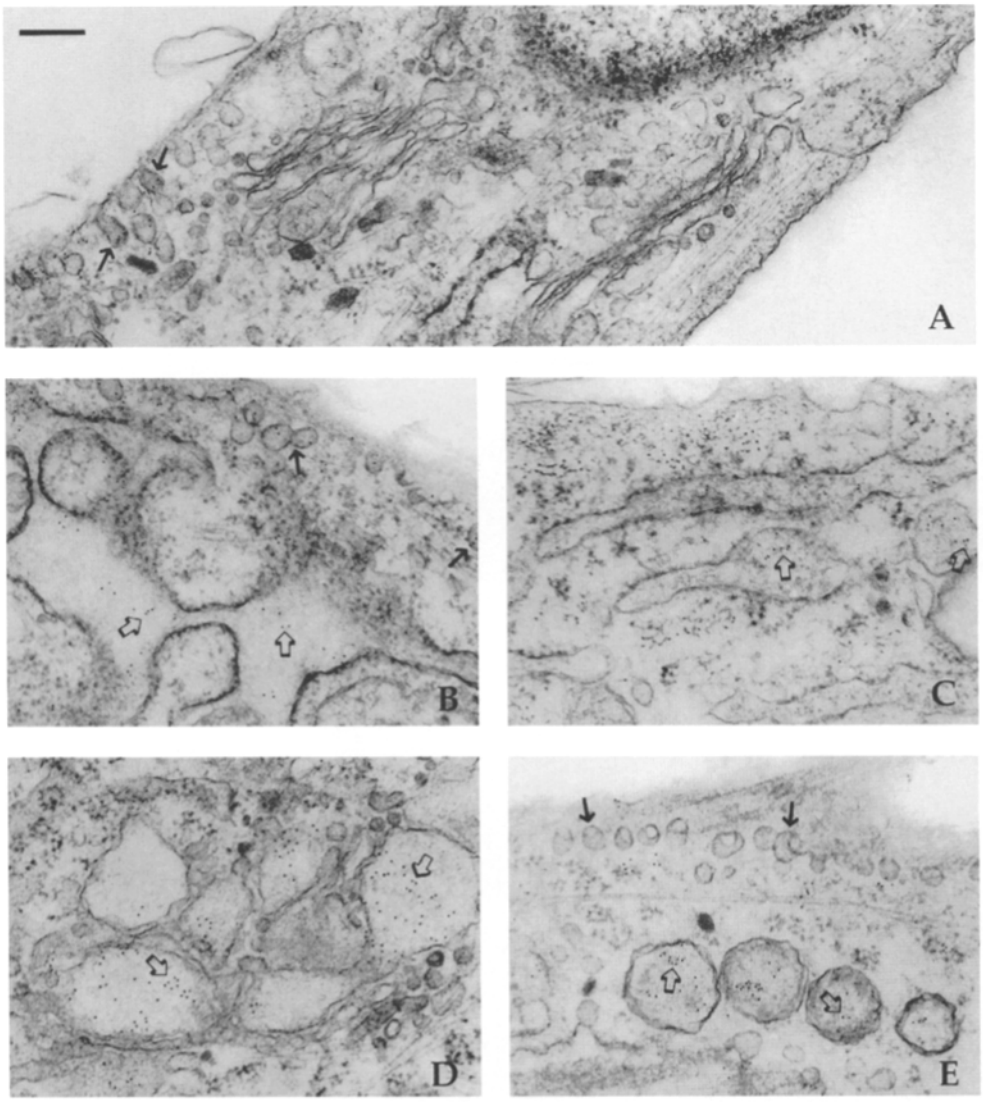


*Figure 7.* Characterization of the caveolin trafficking cycle by immunogold EM. Normal human fibroblasts were cultured in control medium (*A*), for 2 h at 15° before transfer to 37° for 0 (*B*), 20 (*C*), or 40 (*D*) min, or for 1 h in 40 μM nocodazole (*E*). In control cells (*A*) and cells incubated at 15° for 2 h (*B*), most gold particles were found at plasma membrane caveolae (→), although partial redistribution of caveolin to the lumen of the ER (⇒) was seen in cold-blocked cells. Within 20 min after cells were returned to 37°(C), caveolin was evident in the lumens of tubulovesicular structures (⇒), which presumably corresponded to the ERGIC. By 40 min at 37° (D), gold particles (⇒) were abundant within the lumens of swollen Golgi stacks. In nocodazole-treated cells (E), caveolae were readily visible (→), but were nearly devoid of immunogold particles. Instead, most gold particles (⇒) were located within vesicle-like structures that presumably represented the ERGIC. The bar in panel *A* equals 0.5 μm.

although labeling of ER and tubulovesicular structures was more noticeable than in controls (Fig. 7 *B*). Soon after cells that had been incubated for 2 h at 15° were shifted to 37°, the distribution of caveolin changed dramatically. After 20 min at 37°, caveolin was no longer found in caveolae, but instead was located in the lumen of tubulovesicular structures (Fig. 7 *C*). The appearance of these structures was consistent with their identification as ERGIC membranes, particularly in light of the immunofluorescence evidence establishing that caveolin accumulates in the ERGIC shortly after release of cells from 15° (see Fig. 6). By 40 min at 37°, caveolin had moved to the lumens of Golgi stacks, which still appeared swollen as a result of the prior cold block (Fig. 7 *D*). Within 60 min of returning the cells to 37°, most of the caveolin had reached plasma membrane caveolae (data not shown). Finally, in cells incubated for 1 h at 37° in the presence of 40 μM nocodazole the caveolin was in the lumen of vesicles that presumably were part of the ERGIC, and was also associated with caveolae. The caveolae in these nocodazole-treated cells had a normal morphology and were slightly less abundant than in control cells (Fig. 7 *E*).

### *The Half-Life of Caveolin*

Taken together, the data described so far suggest the existence of a constitutive transport cycle in which caveolin moves reversibly between plasma membrane caveolae and the Golgi in normal, unperturbed cells (see Fig. 10 and the Discussion section). This interpretation might be flawed, however, if the half-life of caveolin were short relative to the time periods for which cells were exposed to perturbants such as CO, nocodazole or 15°. If its half-life were short, the caveolin that was observed to move through the ER, ERGIC, and Golgi might simply have been newly synthesized protein traveling through successive compartments of the secretory pathway, rather than pre-existing caveolin undergoing a normal transport cycle.

To resolve this ambiguity, the half-life of caveolin was determined by immunoprecipitation from cells pulsed with [$^{35}$S]methionine and chased with unlabeled methionine. Radiolabeled caveolin was detectable by immunoprecipitation until 20 h of chase. The half-life of caveolin is therefore ~10 h, or about 5 times longer than the longest experiment shown in Figs. 2–7. We also repeated many of the immunofluorescence time course experiments using cells

that were continuously exposed to cycloheximide beginning 1 h before exposure to CO, nocodazole, or 15°. Cycloheximide did not detectably alter any of the immunofluorescence results. Evidently, therefore, the collective results shown in Figs. 2–7 indicate the behavior of pre-existing caveolin, and their interpretation should not be clouded by any newly synthesized caveolin that may have been present in the cells.

### *Biochemical Characterization of the Caveolin Transport Cycle*

The immunofluorescence and immunoelectron microscopic data documented in Figs. 2–7 imply that caveolin travels through the cytoplasm in association with intracellular membranes, and is intraluminal when localized at the ERGIC and Golgi. To investigate caveolin transport by a different approach, the distribution of caveolin was studied in two sets of experiments by biochemical analysis of isolated subcellular fractions. In both cases, cells were treated for 1 h with 50 μg/ml of cycloheximide, after which they were cultured for an additional hour with or without 40 μM nocodazole in the continued presence of cycloheximide. The cells were then homogenized, and postnuclear supernatants were prepared.

The aim of the first group of experiments was to document the movement of caveolin from plasma membrane to internal cellular membranes. Each postnuclear supernatant was fractionated on a Percoll gradient, yielding three distinct fractions (27): cytosol, highly purified plasma membrane, and intracellular membranes (Golgi, ER, lysosomes, endosomes, mitochondria, etc). An aliquot of each fraction containing 50 μg of protein was then analyzed by immunoblotting with anti-caveolin. As illustrated in Fig. 8 *A*, all of the detectable caveolin was in the plasma membrane fraction isolated from control cells. In the case of nocodazole-treated cells, however, caveolin was detected solely in the intracellular membrane fraction. These biochemical results confirm that caveolin redistributes from the plasma membrane to intracellular membranes following treatment of cells with nocodazole.

The next set of experiments was designed to determine whether the redistributed caveolin was located within the lumen of intracellular membranes. First, the postnuclear supernatants were centrifuged at 100,000 $g_{max}$ for 1 h to yield soluble and particulate fractions. Next, each fraction was incubated for 30 min on ice in the presence or absence of trypsin. Finally, all of the fractions were analyzed by anti-caveolin immunoblotting. Fig. 8 *B* demonstrates that caveolin quantitatively cofractionated with particulate membranes in both control and nocodazole-treated cells, consistent with the results shown in Fig. 8 *A*. In addition, Fig. 8 *B* shows that trypsin could fully degrade caveolin when caveolin was associated with the plasma membrane, but not when it was associated with internal cellular membranes unless they first had been solubilized with SDS. These results are consistent with immuno-EM evidence that caveolin is exposed to the cytoplasm when associated with plasma membrane caveolae, but is located within the lumens of intracellular membrane-bounded compartments of nocodazole-treated cells (see Fig. 7).

### *Caveolin Is Not Associated with Endosomes or Lysosomes*

Even though immunofluorescence data indicated an accumulation of caveolin in the ERGIC of nocodazole-treated cells (Figs. 2, 4, and 7), the results of the protease protection experiments (Fig. 8) raised the alternative possibility that nocodazole induces caveolin to be internalized into endosomes. To investigate that possibility, cells were treated with 40 μM nocodazole for 1.5 h, after which they were fixed and stained for double immunofluorescence

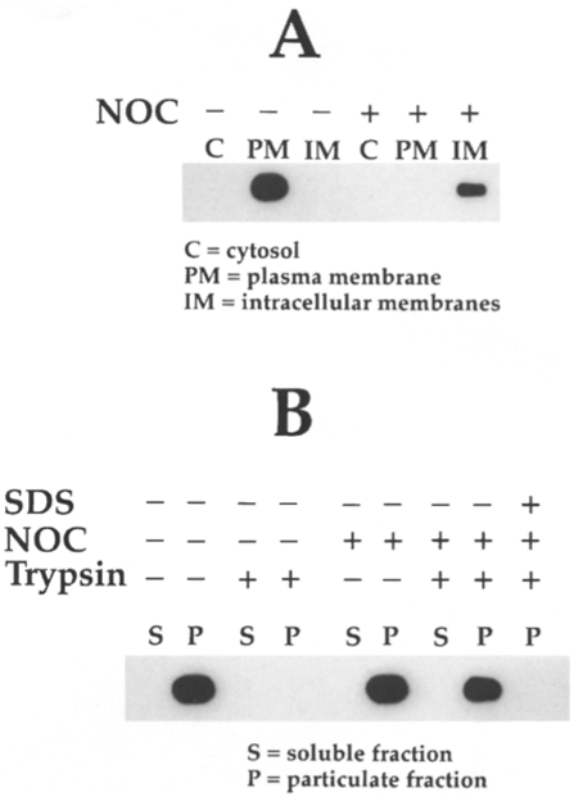


*Figure 8.* Biochemical characterization of the caveolin trafficking cycle. Cells were treated for 1 h with cycloheximide to inhibit protein synthesis, after which they were cultured for an additional hour with or without 40 μM nocodazole in the continued presence of cycloheximide. The cells were then homogenized, and postnuclear supernatants were prepared. (*A*) Postnuclear supernatants were fractionated on Percoll gradient, yielding three distinct fractions (27): cytosol, highly purified plasma membrane, and intracellular membranes (Golgi, ER, lysosomes, endosomes, mitochondria, etc). An aliquot of each fraction containing 50 μg of protein was then analyzed by immunoblotting with anti-caveolin. As shown here, all of the detectable caveolin was in the plasma membrane fraction isolated from control cells. In the case of cells treated with nocodazole (NOC), however, caveolin was detected solely in the intracellular membrane fraction. (*B*) Postnuclear supernatants were centrifuged at 100,000 $g_{max}$ for 1 h to yield soluble and particulate fractions. Each fraction was then incubated for 30 min on ice in the presence or absence of trypsin, and subsequently was analyzed by immunoblotting with anti-caveolin. It is evident that caveolin quantitatively cofractionated with the particulate fraction in both control and nocodazole-treated cells. In addition, trypsin fully degraded caveolin when caveolin was associated with the plasma membrane, but not when it was associated with internal cellular membranes unless they were solubilized with SDS.

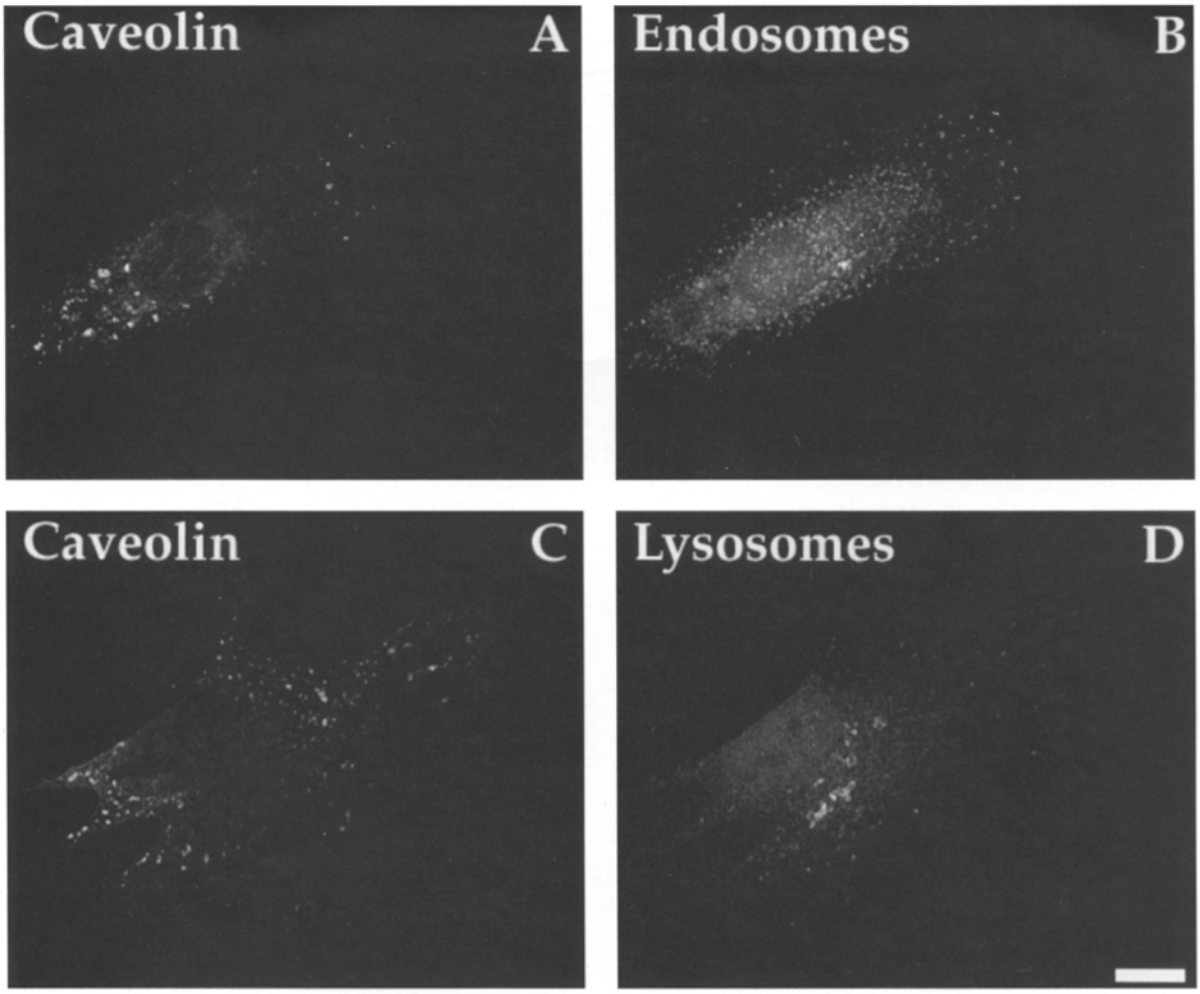


*Figure 9.* Caveolin does not redistribute to endosomes or lysosomes in cells exposed to nocodazole. The distributions of caveolin (*A* and *C*) and an endosomal marker, the LDL receptor (*B*), or a lysosomal marker, cathepsin D (*D*), are shown by double immunofluorescence in normal human fibroblasts cultured in the presence of 40 μM nocodazole for 1.5 h. Note that the distributions of caveolin and the LDL receptor or cathepsin D overlap only marginally. The bar in panel *D* equals 10 μm.

with monoclonal anti-caveolin and a polyclonal antibody to either the LDL receptor or cathepsin D, which served as markers for endosomes and lysosomes, respectively. As shown in Fig. 9, the distributions of caveolin and the LDL receptor or cathepsin D overlapped only marginally in nocodazole-treated cells. These results rule out the possibility that exposure of cells to nocodazole induces caveolin to accumulate preferentially in endosomes or lysosomes. Furthermore, the results are fully consistent with the evidence shown in Figs. 2, 4, and 7 that caveolin is localized in the ERGIC of nocodazole-treated cells.

## *Discussion*

Many structurally and functionally distinct compartments within the secretory and receptor-mediated endocytotic pathways have been found to be dynamic structures whose maintenance depends upon a balance between the influx and efflux of proteins and lipids that are exchanged with adjacent compartments of the pathways. The vehicles for transport between compartments are often tubulovesicular structures that move along MTs. For example, tubulovesicular membranes of the ERGIC are responsible for bidirectional, MT-based transport of material between the ER and the Golgi (10, 11).

The study described here was based on the hypothesis that caveolae, like the ER, the Golgi, and other classes of quasi-stable membrane compartments, are dynamic structures that depend upon MT-based transport to exchange materials with other compartments. Based on the recent finding that CO reversibly causes the resident caveolar protein, caveolin, to relocate from the plasma membrane to the Golgi (28), we decided to explore the possibility that CO had revealed a normal cyclic transport pathway for caveolin.

We found that a cyclic pathway for the trafficking of caveolin through multiple membrane compartments could be detected in cells that were transiently exposed not only to CO, but also to nocodazole or 15°. Regardless of which single perturbant or combination of perturbants were used, a unique overall pathway comprising a unique set of consecutive steps was consistently observed. Dissection of the pathway into distinct, individual steps was possible because each perturbant that was analyzed, CO, nocodazole

and 15°, placed a roadblock at its own signature location within the pathway. Because the same pathway was revealed by three different perturbants whose modes of action are mutually distinct, we strongly favor the hypothesis that a specific cyclic pathway, which is summarized in Fig. 10, is normally followed by caveolin in unperturbed cells.

The initial inward step of the pathway leads caveolin from plasma membrane caveolae to the ER. Incubation of cells at 15° for 2 h apparently blocks this step specifically, because within minutes after cells are returned to 37°, caveolin exits the plasma membrane synchronously and en masse (see Fig. 6). Evidently, this block is effective, but incomplete, because more caveolin was detected by immuno-EM in the ER of cold-blocked cells than of control cells (see Fig. 7). After reaching the ER, caveolin moves next to the ERGIC and then to the Golgi. Passage of caveolin through the two latter compartments was documented throughout the present study by colocalization of caveolin with β-COP, a marker for both the ERGIC and the Golgi. By comparison, caveolin did not colocalize with markers for endosomes or lysosomes after exiting the plasma membrane and ER (see Fig. 9). Because caveolin was able to reach the ERGIC, but not the Golgi, in CO-treated cells that were also exposed to nocodazole (see Fig. 2), or in cells treated with nocodazole alone (see Fig. 4), movement from the ERGIC to the Golgi evidently requires MTs. In contrast, the return of caveolin from the Golgi to the plasma membrane apparently does not require MTs, because nocodazole did not block this step of the cycle in cells that were released from either CO (see Fig. 3) or a 15° temperature block (data not shown). It is also noteworthy that the Golgi-to-cell surface step does not appear to occur via the ERGIC, because caveolin did not colocalize with β-COP during this stage of the cycle (see Fig. 3).

In light of the fact that ~90% of the caveolin recognized by the monoclonal anti-caveolin used throughout this study is localized in caveolae at steady state in unperturbed cells (7, 19), we propose that the rate-limiting step in the normal cycle is movement of caveolin from caveolae to the ER. In CO-treated cells (see Fig. 2), however, the rate-limiting step appears to be transport from the Golgi back to the plasma membrane, because caveolin accumulates in the Golgi or post-Golgi vesicles after exposure of cells to CO (28). While this could be due to CO blocking transport at the Golgi-to-plasma membrane step, it might alternatively reflect, as we suspect, a CO-mediated acceleration of caveolin movement off of the plasma membrane. Perhaps oxidized caveolar cholesterol, which increases dramatically after cells are treated with CO (28), stimulates movement of caveolin from caveolae into the ER. The entire cycle has been observed in cells treated with cycloheximide (see Fig. 8, and [28]), indicating that whatever contributions newly synthesized caveolin may have made to the data documented in Figs. 2–7, the issue of caveolin synthesis is irrelevant to the model depicted in Fig. 10. Finally, it must be emphasized that the existence of transport steps not specified in the model, such as direct movement of caveolin from the ER to the plasma membrane, cannot be ruled out by the data that are currently available.

The pathway summarized in Fig. 10 is consistent with the existing data for only one component of caveolae, the coat-associated protein, caveolin. There is a very recent report that apparently intact caveolae can be induced to move from the plasma membrane to the cell center by a MT-dependent process after exposure of cells to the protein phosphatase inhibitor, okadaic acid, in the presence of hypertonic medium (16). Our evidence implies that bulk transport of caveolae between the cell surface and the Golgi does not normally occur, but does not rule out the possibility that multiple components of caveolae follow the same bidirectional pathway traveled by caveolin.

What functions could be served by the cyclic transport of caveolin? One possibility worthy of serious consideration is that caveolin carries exogenous fatty acids from their sites of uptake at the plasma membrane to the ER, where they are converted to membrane lipids. Underscoring this possibility is the recent finding that caveolin binds a long chain fatty acid with high affinity (Anderson, R. G. W., unpublished observations). In light of this discovery, it will be worthwhile to examine whether fatty acids and the lip-

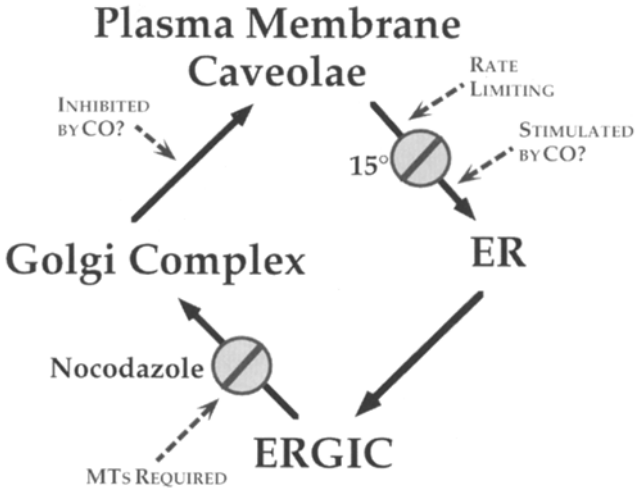


*Figure 10.* A model for the constitutive trafficking of caveolin. The collective data presented in this report suggest that caveolin normally undergoes constitutive cycling between plasma membrane caveolae and the Golgi complex. The cycle evidently leads sequentially from caveolae to the ER, the ERGIC, the Golgi, and finally back to the plasma membrane. Because most caveolin is localized in caveolae at steady state in unperturbed cells (see Figs. 2 *A* and 4 *A*), it seems likely that the rate limiting step in the normal cycle is movement from caveolae to the ER. This step seems to be inhibited when cells are incubated at 15°, because return of cells to 37° leads to the rapid, synchronous movement of caveolin through the cycle (see Fig. 6). One step, from the ERGIC to the Golgi, is blocked by nocodazole, and therefore requires MTs (see Figs. 2 and 4). Transport from the Golgi to the plasma membrane is MT independent, and occurs via apparent vesicular intermediates that do not colocalize with β-COP, and therefore seem to be distinct from the ERGIC (see Fig. 3). The buildup of caveolin in the Golgi of CO-treated cells implies that the Golgi-to-plasma membrane step is rate limiting in the presence of CO. This could be due to CO accelerating the caveolae-to-ER step or inhibiting the Golgi-to-plasma membrane step. Presently available data do not allow us to discriminate between these possibilities. Finally, while the model shown here is consistent with present evidence, it does not exclude additional steps that theoretically could occur, such as direct bidirectional transport between the plasma membrane and the ER.

ids into which they are converted are cotransported with caveolin as it cycles between caveolae and the Golgi. Bidirectional transport of caveolin could also serve the purpose of returning resident Golgi proteins that escape to the plasma membrane because they are incorporated into secretory vesicles that are delivered to the cell surface.

Regardless of what functions may be served by cyclic transport between caveolae and the Golgi, the results presented here emphasize a novel protein transport pathway that coincides, at least in part, with the route followed by nascent secretory proteins and lipids. Not only do those newly synthesized products travel successively through the ER, the ERGIC and the Golgi, before travelling to the plasma membrane in Golgi-derived vesicles, but so too does at least one resident protein of cell surface caveolae. That protein, caveolin, appears to follow this route constitutively and, we presume, repetitively. The challenge now is to learn why this occurs, and to determine whether other caveolar components undergo similar cycling. Several other important issues that are raised by the present study warrant attention in the near future. Foremost among those issues are the identity of the MT motor responsible for moving caveolin from the ERGIC to the Golgi, the MT-independent mechanism by which caveolin moves from the Golgi to the plasma membrane, and the mechanism by which caveolin is converted between a cytoplasmically oriented membrane protein at the cell surface and an intraluminal protein when associated with intracellular membranes.

The authors would like to thank Bill Donzell for assistance with tissue culture, and Drs. John Glenney, Jennifer Lippincott-Schwartz, Thomas Kreis, Hans-Peter Hauri, Eric Berger, Joe Goldstein, and Bill Brown for providing antibodies that were essential for this study.

This work was supported by grants from the National Institutes of Health (NIH) (NS30485), the American Cancer Society (CB-58C) and the Robert A. Welch Foundation (I-1236) to G. S. Bloom, and from the NIH (HL20948, GM 43169, and GM 15631) and the Perot Family Foundation to R. G. W. Anderson.

Received for publication 24 April 1995 and in revised form 27 September 1995.

### *References*

1. Anderson, R. G. W. 1993. Plasmalemmal caveolae and GPI-anchored membrane proteins. *Curr. Opin. Cell Biol.* 5:647–652.
2. Anderson, R. G. W., B. A. Kamen, K. G. Rothberg, and S. W. Lacey. 1992. Potocytosis: sequestration and transport of small molecules by caveolae. *Science (Wash. DC).* 255:410–411.
3. Berger, E. G., U. Müller, E. Aegerter, and G. J. Strous. 1987. Biology of galactosyltransferase: recent developments. *Biochem. Soc. Trans.* 15:610–613.
4. Brown, D. A., and J. K. Rose. 1992. Sorting of GPI-anchored proteins to glycolipid-enriched membrane subdomains during transport to the apical cell surface. *Cell.* 68:533–544.
5. Chang, W. J., Y. S. Ying, K. G. Rothberg, N. M. Hooper, A. J. Turner, H. A. Gambliel, J. De Gunzburg, S. M. Mumby, A. G. Gilman, and R. G. W. Anderson. 1994. Purification and characterization of smooth muscle cell caveolae. *J. Cell Biol.* 126:127–138.
6. Duden, R., G. Griffiths, R. Frank, P. Argos, and T. E. Kreis. 1991. β-COP, a 110 kD protein associated with non-clathrin–coated vesicles and the Golgi complex, shows homology to b-adaptin. *Cell.* 64:649–665.
7. Dupree, P., R. G. Parton, G. Raposo, T. V. Kurzchalia, and K. Simons. 1993. Caveolae and sorting in the trans-Golgi network of epithelial cells. *EMBO (Eur. Mol. Biol. Org.) J.* 12:1597–1605.
8. Ho, W. C., V. J. Allan, G. van Meer, E. G. Berger, and T. E. Kreis. 1989. Reclustering of scattered Golgi elements occurs along microtubules. *Eur. J. Cell Biol.* 48:250–263.
9. Laemmli, U. K. 1970. Cleavage of structural proteins during the assembly of the head of bacteriophage T4. *Nature (Lond.).* 227:680–685.
10. Lippincott-Schwartz, J., N. B. Cole, A. Marotta, P. A. Conrad, and G. S. Bloom. 1995. Kinesin is the motor for microtubule-mediated Golgi-to-ER membrane traffic. *J. Cell Biol.* 128:293–306.
11. Lippincott-Schwartz, J., J. G. Donaldson, A. Schweizer, E. G. Berger, H.-P. Hauri, L. C. Yuan, and R. D. Klausner. 1990. Microtubule-dependent retrograde transport of proteins into the ER in the presence of brefeldin A suggests an ER recycling pathway. *Cell.* 60:821–836.
12. Lisanti, M. P., P. E. Scherer, Z. Tang, and M. Sargaicomo. 1994. Caveolae, caveolin and caveolin-rich membrane domains: a signalling hypothesis. *Trends Cell Biol.* 4:231–235.
13. Matteoni, R., and T. E. Kreis. 1987. Translocation and clustering of endosomes and lysosomes depends on microtubules. *J. Cell Biol.* 105:1253–1265.
14. Palade, G. E., and R. R. Bruns. 1968. Structural modulations of plasmalemmal vesicles. *J. Cell Biol.* 37:633–649.
15. Park, J. E., R. K. Draper, and W. J. Brown. 1991. Biosynthesis of lysosomal enzymes in cells of the End3 complementation group conditionally defective in endosomal acidification. *Somat. Cell Mol. Gen.* 17:137–150.
16. Parton, R. G., B. Joggerst, and K. Simons. 1994. Regulated internalization of caveolae. *J. Cell Biol.* 127:1199–1215.
17. Pepperkok, R., J. Scheel, H. Horstmann, H. P. Hauri, G. Griffiths, and T. E. Kreis. 1993. β-COP is essential for biosynthetic membrane transport from the endoplasmic reticulum to the Golgi complex invivo. *Cell.* 74:71–82.
18. Rogalski, A. A., and S. J. Singer. 1984. Associations of elements of the Golgi apparatus with microtubules. *J. Cell Biol.* 99:1092–1100.
19. Rothberg, K. G., J. E. Heuser, W. C. Donzell, Y. -S. Ying, J. R. Glenney, and R. G. W. Anderson. 1992. Caveolin, a protein component of caveolae membrane coats. *Cell.* 68:673–682.
20. Saraste, J., and E. Kuismanen. 1984. Pathways of protein sorting and membrane traffic between the rough ER and the Golgi complex. *Semin. Cell Biol.* 3:343–355.
21. Sargiacomo, M., M. Sudol, Z. Tang, and M. P. Lisanti. 1993. Signal transducing molecules and glysosyl-phosphatidylinositol-linked proteins form a caveolin-rich insoluble complex in MDCK cells. *J. Cell Biol.* 122:789–807.
22. Scheel, J., R. Matteoni, T. Ludwig, B. Hoflack, and T. E. Kreis. 1990. Microtubule depolymerization inhibits transport of cathepsin D from the Golgi apparatus to lysosomes. *J. Cell Sci.* 96:711–720.
23. Schweizer, A., J. A. M. Fransen, T. Baechi, L. Ginsel, and H.-P. Hauri. 1988. Identification by a monoclonal antibody of a 53-kD protein associated with a tubulovesicular compartment at the *cis*-side of the Golgi apparatus. *J. Cell Biol.* 107:1643–1653.
24. Schweizer, A., J. A. M. Fransen, K. Matter, T. E. Kreis, L. Ginsel, and H.-P. Hauri. 1990. Identification of an intermediate compartment involved in protein transport from endoplasmic reticulum to Golgi apparatus. *Eur. J. Cell Biol.* 53:185–196.
25. Serafini, T., G. Stenbeck, A. Brecht, F. Lottspeich, L. Orci, J. E. Rothman, and F. T. Wieland. 1991. A coat subunit of Golgi-derived non-clathrin-coated vesicles with homology to the clathrin-coated vesicle coat protein b-adaptin. *Nature (Lond.).* 349:215–220.
26. Smart, E. J., D. C. Foster, Y. -S. Ying, B. A. Kamen, and R. G. W. Anderson. 1994. Protein kinase C activators inhibit receptor-mediated-potocytosis by preventing internalization of caveolae. *J. Cell Biol.* 124:307–313.
27. Smart, E. J., Y.-S. Ying, C. Mineo, and R. G. W. Anderson. 1995. A detergent-free method for purifying caveolae membrane from tissue culture cells. *Proc. Natl. Acad. Sci. USA.* 92:10104–10108.
28. Smart, E. J., Y. S. Ying, P. A. Conrad, and R. G. W. Anderson. 1994. Caveolin moves from caveolae to the Golgi apparatus in response to cholesterol oxidation. *J. Cell Biol.* 127:1185–1197.
29. Swanson, J. A., A. Bushnell, and S. C. Silverstein. 1987. Tubular lysosome morphology and distribution within macrophages depend on the integrity of cytoplasmic microtubules. *Proc. Natl. Acad. Sci. USA.* 84:1921–1925.
30. Terasaki, M., L. B. Chen, and K. Fujiwara. 1986. Microtubules and the endoplasmic reticulum are highly interdependent structures. *J. Cell Biol.* 103:1557–1568.
31. Thyberg, J., and S. Moskalewski. 1985. Microtubules and the organization of the Golgi complex. *Exp. Cell Res.* 159:1–16.
32. Towbin, H., T. Staehelin, and J. Gordon. 1979. Electrophoretic transfer of proteins from polyacrylamide gels to nitrocellulose sheets: procedure and some applications. *Proc. Natl. Acad. Sci. USA.* 76:4350–4354.
33. Turner, J. R., and A. M. Tartakoff. 1989. The response of the Golgi complex to microtubule alterations: roles of metabolic energy and membrane traffic in Golgi complex organization. *J. Cell Biol.* 109:2081–2088.
34. Vallee, R. B., and G. S. Bloom. 1983. Isolation of sea urchin egg microtubules using taxol and identification of mitotic spindle microtubule-associated proteins with monoclonal antibodies. *Proc. Nat. Acad. Sci. USA.* 80: 6259–6263.
35. Ying, Y.-S., R. G. W. Anderson, and K. G. Rothberg. 1992. Each caveolae contains multiple glycosyl-phosphatidylinositol anchored membrane proteins. *Cold Spring Harbor Symp. Quant. Biol.* 57:593–604.